Intrinsically limited critical temperatures of highly doped $Ga_{1-x}Mn_xAs$ thin films

Kh. Khazen, H. J. von Bardeleben, and J. L. Cantin
Institut de Nanosciences de Paris, Université Paris 6, UMR 7588 au CNRS, 140 rue de Lourmel, 75015 Paris, France

A. Mauger
Institut de Minéralogie et Physique des Milieux Condensés (IMPMC), Université Paris 6, UMR 7590 au CNRS, 140 rue de Lourmel, 75015 Paris, France

L. Chen and J. H. Zhao
State Key Laboratory for Superlattices and Microstructures, Institute of Semiconductors, Chinese Academy of Sciences, P.O. Box 912, Beijing 100083, China

(Received 15 January 2010; revised manuscript received 19 April 2010; published 2 June 2010)

$Ga_{1-x}Mn_xAs$ films with exceptionally high saturation magnetizations of ≈ 100 emu/cm^3 corresponding to effective Mn concentrations of $x_{eff} \approx 0.10$ still have a Curie temperature T_C smaller than 195 K contradicting mean-field predictions. The analysis of the critical exponent β of the remnant magnetization—$\beta = 0.407(5)$—in the framework of the models for disordered /amorphous ferromagnets suggests that this limit on T_C is intrinsic and due to the short range of the ferromagnetic interactions resulting from the small mean-free path of the holes. This result questions the perspective of room-temperature ferromagnetism in highly doped GaMnAs.

DOI: 10.1103/PhysRevB.81.235201 PACS number(s): 75.50.Pp, 75.40.−s, 75.60.Ej

I. INTRODUCTION

Theoretical predictions of Curie temperatures close or above room temperature for highly ($x \geq 0.10$) doped $Ga_{1-x}Mn_xAs$ thin films[1] have initiated intensive research to elaborate highly doped layers, which would allow interesting applications in spintronics. According to mean-field predictions the critical temperature T_C^{MF} of $Ga_{1-x}Mn_xAs$ layers is

$$T_C^{MF} = \frac{N_{Mn} S(S+1)}{3k_B} \cdot \frac{J_{pd}^2 \chi_f}{(g\mu_B)^2}. \quad (1)$$

With N_{Mn} the density of the Mn^{2+} ions that participate to the ferromagnetic ordering, S the Mn^{2+} spin, J_{pd} the p-d exchange integral, and χ_f the free carrier susceptibility, other notations are conventional. With typical values for $Ga_{1-x}Mn_xAs$ and $x=0.05$ this expression predicts already a T_C^{MF} of 125 K, in agreement with many reported experimental results. For $x=0.10$ a value close to room temperature is expected assuming negligible electrical compensation. Different corrections[2–6] have been added to this model, which, however cannot explain the limit of T_C to approximately 195 K, which is still the highest value reported.[7]

The successful growth of highly doped layers with x up to 0.2 have been reported by different groups[7–12] but the deceivingly small saturation magnetization values of these films show that only a fraction of the Mn dopant is magnetically active and their effective Mn concentration x_{eff} is only in the range 0.05–0.07. They are thus not suited to test the mean-field predictions of T_C in the case of high doping. The distinction between effective and total Mn concentrations is related to the incorporation of Mn not only in substitution for Ga but also at interstitial lattice sites where they reduce both the magnetization and free carrier concentration of the films. In the past, a possible overestimation of T_C by the mean-field approximation due to the neglect of long-wavelength collective fluctuations has been considered.[13] However, this effect is compensated by enhancement of the spin stiffness by the strong spin-orbit coupling inside the valence band,[14] so that the mean-field approximation seemed quantitatively correct in $Ga_{1-x}Mn_xAs$.[15]

In the present work, we have investigated the magnetic properties of two samples with exceptionally high saturation magnetizations of 85 and 105 emu/cm^3 corresponding to effective Mn concentrations $x_{eff}=0.08$ and $x_{eff}=0.10$. They are thus well suited to test the mean-field predictions. In order to exclude the presence of secondary phases which can easily precipitate at such high doping levels we have first characterized these films by ferromagnetic resonance (FMR) spectroscopy. This spectroscopy allows the detection of ferromagnetic precipitates even of nanometer size, which can easily escape detection by x-ray analysis. The FMR measurements allow us to determine also the magnetic anisotropy constants and the easy axis for magnetization in the 4 K to T_C temperature range.

To address the problem of the limited T_C, the critical exponent β of the magnetization has been investigated by measurements of the magnetization in the vicinity of T_C. This is a static property that gives some insight in the nature of the magnetic interactions. The results are analyzed in the framework of disordered ferromagnets, and suggest that the limit in T_C may be due to the fact that the ferromagnetic interactions are short range, due to the small mean-free path of the carriers.

II. SAMPLE GROWTH AND CHARACTERIZATION

$Ga_{1-x}Mn_xAs$ layers were grown at 200 °C by low-temperature (LT) molecular beam epitaxy (MBE) on (100) oriented GaAs substrates. To avoid the precipitation of secondary phases the layer thickness was limited to <15 nm. The layers were capped with a thin LT MBE GaAs layer and have been annealed at 150 °C for 16 h. The two layers in-

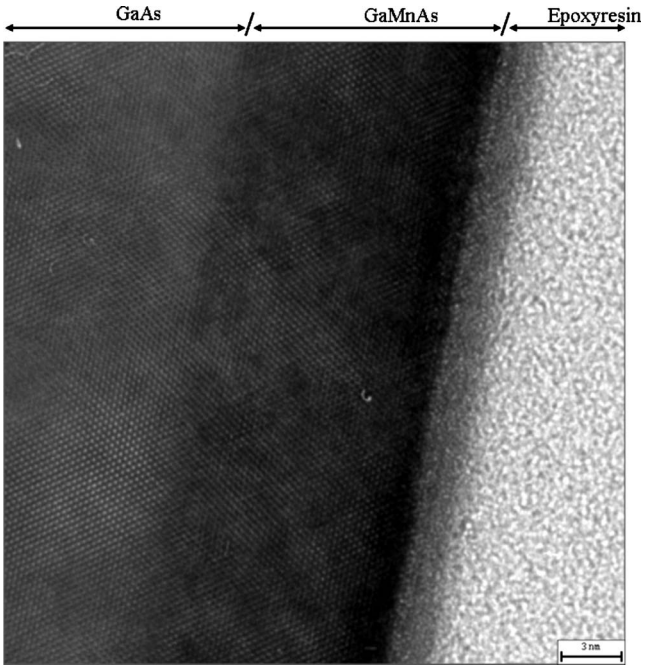

FIG. 1. High-resolution transmission electron microscopy image of sample A.

vestigated in this work have, respectively, total Mn concentrations of (A) $x=0.25$, thickness 15 nm and (B) $x=0.24$, thickness 7 nm. The thickness of the layers, targeted from calibrated growth conditions have been directly verified by x-ray reflection (XRR), high-resolution x-ray diffraction (HRXRD), and transmission electron microscopy (TEM) (Figs. 1 and 2). The results obtained are in good agreement with these values: 14 nm (TEM); 14 nm (HRXRD), and 14.5 nm (XRR) for sample A and 7 nm (HRXRD) for sample B. Both layers are metallic with an electrical resistivity of $\rho_{xx} \approx 5$ mΩ cm (Fig. 3).

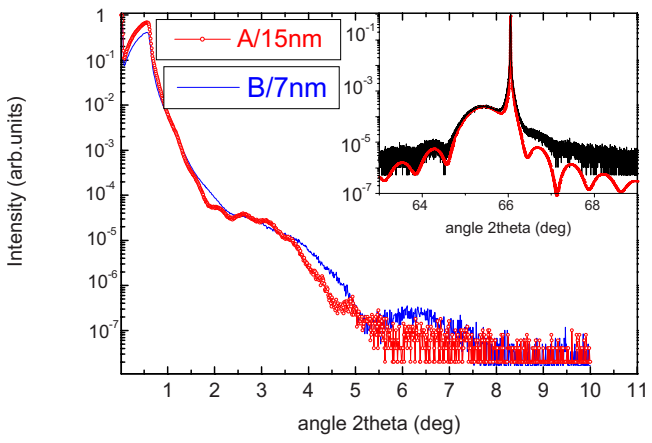

FIG. 2. (Color online) X-ray reflection spectra of sample A (red dots) and B (blue line). The thickness of the layers is obtained from the analysis of the Kiessig fringes. The intensity is plotted on a logarithmic scale. Inset: high-resolution x-ray diffraction spectrum (black line) and its simulation (red dotted line) for sample A. The intensity is plotted on a logarithmic scale.

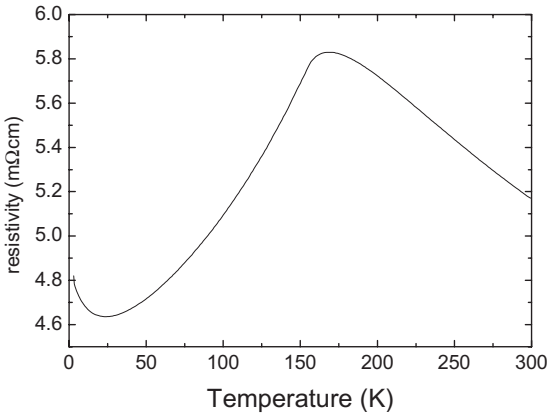

FIG. 3. Electrical resistivity ρ_{xx} (mΩ cm) as a function of temperature (kelvin) for sample A.

III. FMR RESULTS

First the samples have been characterized by ferromagnetic resonance.[16,17] In Fig. 4, we show a typical X-band spectrum of sample A. The spectra of sample B are very similar. We observe only the uniform mode single line spectrum of the ferromagnetic GaMnAs phase. A large field scan from 0 to 18 kOe with increased gain gives no evidence for the presence of any ferromagnetic precipitate such as MnAs.

The magnetocrystalline anisotropy constants have been determined from the angular variations in the uniform mode spectrum in the (110) and (001) planes (Fig. 3) using the Smit Beljers formalism[18] and the following free-energy density expression F,

$$F = -MH[\cos\theta\cos\theta_H + \sin\theta\sin\theta_H\cos(\phi-\phi_H)] - 2\pi M^2\sin^2\theta - K_{2\perp}\cos^2\theta - \frac{1}{2}K_{4\perp}\cos^4\theta - \frac{1}{2}K_{4\parallel}\frac{3+\cos 4\phi}{4}\sin^4\theta - K_{2\parallel}\sin^2\theta\sin^2\left(\phi-\frac{\pi}{4}\right), \quad (2)$$

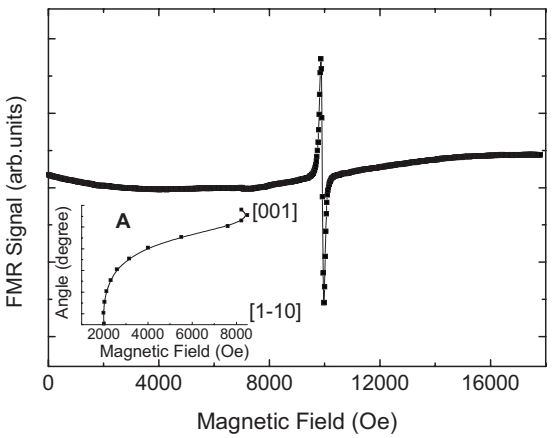

FIG. 4. Large scale FMR spectrum at $T=60$ K for $H\|[001]$ for sample A; inset: angular variation in the FMR resonance field for an out-of-plane variation (black squares), a fit with $g=2.00$, and the anisotropy constants given in Table I.

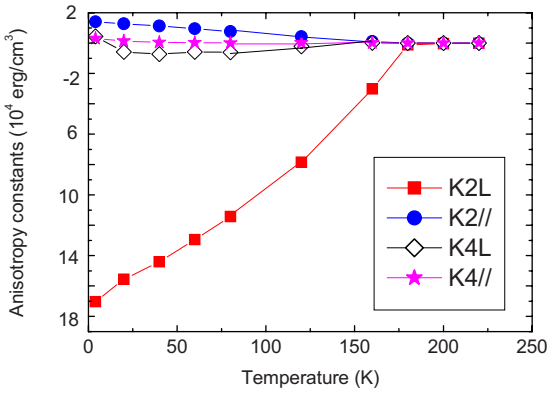

FIG. 5. (Color online) Magnetic anisotropy constants K of second and fourth order ($\parallel$ in plane, $\perp$ out of plane) as a function of temperature determined from the angular variation in the FMR spectra of sample A.

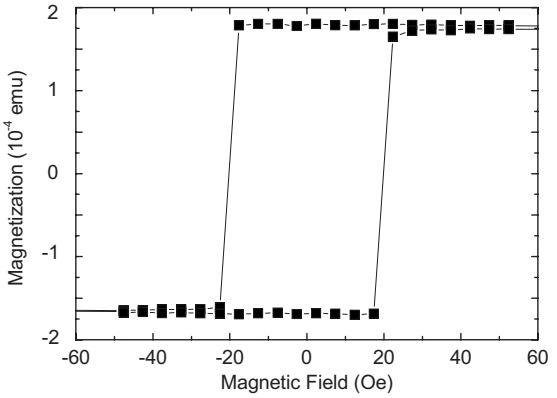

FIG. 6. Magnetization hysteresis curve $M(H)$ for sample A at 4 K, $H\parallel[1\bar{1}0]$.

where θ, ϕ are the azimutal and polar angles, M_S the saturation magnetization, γ the gyromagnetic ratio, ω the microwave frequency, and K the second- and fourth-order anisotropy constants.

The Landé g factor and the anisotropy constants (Fig. 5) are determined from the fit of the angular variation in the resonance fields for temperatures T in the range $4\ \mathrm{K} < T < T_C$. The dominant anisotropy constant is $K_{2\perp}$ with a value of $-170\,300\ \mathrm{erg/cm^3}$ at $T=4$ K. This is twice the value observed in standard ($x=0.05$) layers (Table I). It should be related to the presence of Mn interstitials and possibly As antisites since both of them are known to expand the lattice constant. The in-plane anisotropy is equally modified as compared to standard $x=0.05$ layers. The FMR results show that the easy axis of magnetization is $[1\bar{1}0]$ in the entire range from 4 K to T_C with no reorientation.

The X-band FMR linewidths are generally dominated by inhomogeneous broadening, and are small in these films ($\approx$50 Oe at 20 K), which proves their excellent magnetic homogeneity. Typical linewidths previously reported for $x=0.05$-doped state-of-the-art layers were in the 100–300 Oe range. The total FMR linewidth is determined by two contributions, an inhomogeneous sample quality dependent part and a homogeneous intrinsic part.[19] Our results show an inhomogeneous linewidth of 25 Oe at $T=20$ K, which proves that the layers are of exceptional magnetic homogeneity, with no gradient in the Mn concentrations and no Mn clustering effects.

IV. MAGNETIC PROPERTIES

The magnetization curves $M(H)$ of these films have been measured with the magnetic field H applied along the easy axis $[1\bar{1}0]$. In thick films the determination of the spontaneous magnetization M_S that must be used for scaling may be difficult as the formation of magnetic domains reduces the magnetization to a remnant magnetization $M_R < M_S$. The great advantage associated with the thin-film geometry here is that the films are single domain. This is evidenced by the squarelike shape of the hysteresis curves $M(H)$ (Fig. 6), which show that $M_R = M_S$. We assume that this relationship holds at all temperatures and use M_R instead of M_S in our scaling analysis.

TABLE I. Magnetic anisotropy constants at $T=4$ K determined by FMR in sample A and comparison with typical values in a $x_{eff}=0.05$ $Ga_{1-x}Mn_xAs$ 50 nm thick film on (100) GaAs.

	$K_{2\perp}$ (erg cm^{-3})	$K_{2\parallel}$ (erg cm^{-3})	$K_{4\perp}$ (erg cm^{-3})	$K_{4\parallel}$ (erg cm^{-3})
$x_{eff}=0.08$	−170300	14030	4402	3305
Standard $x_{eff}=0.05$	−80000	3000	−5000	6000

The coercive field for $H\parallel[1\bar{1}0]$ at 4 K is 20 Oe. The temperature dependence of the magnetization $M_R(T)$ is shown in Fig. 7. The effective Mn concentrations deduced from M_S at 4.2 K are $x_{eff}=0.08$ and $x_{eff}=0.10$, and the Curie temperatures are 168 K and 148 K, respectively. An insight in the difference of the magnetic properties with respect to the mean-field predictions is provided by the analysis of the magnetization $M_R(T)$, in the critical regime below T_C where $M_R(T)$ takes the form $M_R(T) \propto t^{\beta}$, with $t=(T_C-T)/T_C$ the reduced temperature. We show in Fig. 8 the variations in $M_R(t)/M_{0.13}$ as a function of t in a log-log plot. $M_{0.13}$ is the magnetization at a temperature $|t|=0.13$ chosen arbitrarily to normalize the data of both samples that can then be plotted on the same "universal" curve. The temperature range investigated is broad enough to evidence the reduced Ginzburg temperature $|t_g|$ above which the classical (mean-field) expo-

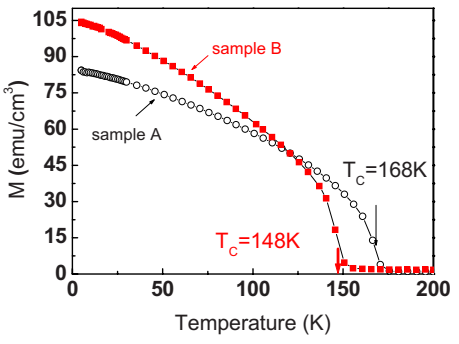

FIG. 7. (Color online) Magnetization M_R as a function of temperature for samples A (open black circles) and B (red, full squares).

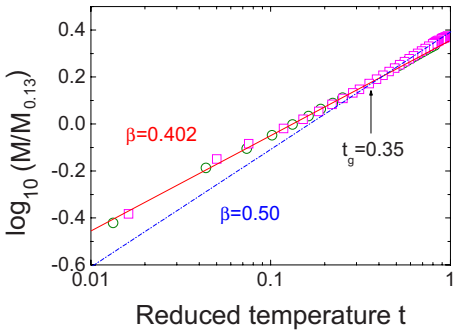

FIG. 8. (Color online) Reduced magnetization $M_R(t)/M_R(t=0.13)$ as a function of the reduced temperature t plotted on a logarithmic scale for samples A (black circles) and B (red squares). The red line corresponds to the critical exponent β and the dotted blue line to the classical exponent 0.5 on both sides of the Ginzburg temperature.

nent 0.5 is observed. We find $|t_g|=0.35$, and in the range $|t|<|t_g|$, $\beta=0.407(5)$ for both samples. This value is slightly larger but compatible with the value derived for a sample with comparable Mn doping[7] since the exponent was estimated with a broad uncertainty (in the range 0.3–0.4). We obtain the same exponent for both films although their thickness differs by a factor 2, so that size effects are negligible, and β is the "bulk" exponent. In the case of the three-dimensional (3D)-Heisenberg model where the interactions are confined to nearest neighbors only, β ranges from 0.35 for $S=1/2$ to 0.378 for $S=\infty$.[20] Such a small exponent in the range 0.37–0.38 is commonly observed in crystalline ferromagnets,[21–23] in agreement with the general theoretical expectation that such homogeneous ferromagnets should belong to the class of universality of 3D-Heisenberg systems.[24] The enhancement of β is characteristic of amorphous ferromagnets, such as $(Fe_{0.4}Ni_{0.6})_{75}P_{16}B_6Al_3$, where $\beta=0.40$,[25,26] $Fe_{32}Ni_{36}Cr_{14}P_{12}B_6$,[27] and $Fe_{10}Ni_{70}B_{19}Si$,[28] where $\beta=0.42$, for instance. The similarity in the values of β in our system is due to the fact that both our system and amorphous materials belong to the same family of disordered magnetic systems. The only difference is that the randomness in amorphous material is structural while in $Ga_{1-x}Mn_xAs$ it is generated by spin dilution. This randomness has major effects, such as the smearing out of the Friedel oscillations of the interaction mediated by the free carriers, hidden behind the derivation of Eq. (1).[29] We find here that the effect on the critical behavior is also important.

V. DISCUSSION

Several models that have been proposed to explain the enhancement of β in random ferromagnets. In particular, a single cluster defect of 2^3 missing spins has been introduced in the spin-diluted Heisenberg ferromagnet,[30] inducing a crossover from $\beta=0.33$ to $\beta=0.41$ as the correlation length becomes smaller than the length of the defect.[31] The antiferromagnetic clusters associated to the presence of Mn in interstitial might be assimilated to the "clusters of missing spins" in this model.

We have analyzed the magnetization data within the scaling approach of phase transitions. Both samples have the same value of $\beta=0.407(5)$, although their Curie temperatures are markedly different, which indicates that the value of β is robust, and that the reduced temperature t is a pertinent variable. This is commonly observed in disordered ferromagnets. For instance, despite the changes in T_C in amorphous $(Fe_xNi_{1-x})_{75}P_{16}Al_3$, the value of $\beta\sim0.4$ was observed consistently.[25] Nevertheless, this method is fully justified for a single T_C value only. The effect of a distribution ΔT_C has been taken into account in the study of $La_{2/3}Ca_{1/3}MnO_3$, a material in which ΔT_C is particularly large because it is a randomly doped mixed valence system.[32] But even in this extreme case the power law with critical exponent analysis is recovered and the exponent β could be determined. However, we should keep in mind that the neglect of the distribution of T_C may influence the determination of β so that the numerical value of β should not be taken as a criterion to define a class of universality. The broad dispersion of the values of β in the whole range $0.36\leq\beta\leq0.5$ met in the disordered ferromagnets is another evidence that the disorder affects β differently, according to the topology of the disorder at all the length scales. The use of the scaling approach in amorphous ferromagnets has been justified by the fact that the magnetic transition is rather sharp, in agreement with the predictions from the renormalization-group approach.[33] The pertinence of this approach is confirmed by the fact that the static scaling relation between critical exponents $\delta=1+\gamma/\beta$ (in standard notations) is observed whenever the critical exponents δ and γ have been measured in amorphous ferromagnets.[34,35] We do assume that the same scaling approach is justified in the GaMnAs system, in which the ferromagnetic transition is also sharp, because the FMR experiments have shown that the samples are remarkably homogeneous.

The magnetic anisotropy cannot explain the value of β. For instance, there is only a small modification of the critical exponents due to the dipolar interactions for isotropic Heisenberg ferromagnets.[36] In the Ising model, β is even smaller, with $\beta=0.312$.[37] The larger value of β is thus attributable to the intrinsic magnetic disorder arising from spin-dilution effect plus eventually magnetic defects such as Mn in interstitial positions.

The disorder, however, is not sufficient to explain our results. The random ferromagnet with infinite range interactions has mean-field critical exponents so that $\beta=0.5$.[38] The value of β intermediate between the mean-field exponent and that of the 3D-Heisenberg model is thus also linked to the short range of the ferromagnetic interactions. Using a self-consistent Monte Carlo procedure, Binder *et al.*[39] have shown that the inclusion of next-nearest-neighbor (nnn) exchange ($J_2=5J_1$) leads to an increase in β by 0.06 with respect to the 3D-Heisenberg case (where the interaction is confined to the exchange J_1 nn) only. An interaction restricted to nnn is thus sufficient to account for a value of β close to the value that we have observed in our material.

An exchange mediated via the free carriers (holes in the occurrence) is usually assumed to be infinite, like in the Ruderman-Kittel-Kasuya-Yoshida interaction, for instance. However, we should keep in mind that the holes are not

"free" since their mean-free path λ is finite. Then a hole will lose the memory of its spin polarization when it will be scattered and cannot propagate the spin polarization at a distance significantly larger than λ. This effect has been investigated by De Gennes[40] who has found that it has severe effects on the magnetic properties of metals. The effect is more dramatic in our samples since λ is much smaller. A rough estimate of λ can be obtained in a simple spherical model (instead of the full calculation from the Kohn-Luttinger Hamiltonian that would be required for a quantitative estimate). Then, $\lambda = v_F \tau$ with τ the relaxation time and $v_F = [\hbar(3\pi^2 p)^{1/3}]/m$ the velocity of the holes at the Fermi energy. τ can be estimated from the electronic resistivity ρ according to the formula $\tau = m/(pe^2\rho)$. For an effective mass of the holes $m = 0.45 m_0$ and hole concentration $p \approx 5 \times 10^{20}$ cm^{-3} that are typical values for our samples, and taking into account the experimental value of their resistivity, $\rho \approx 5$ mΩ cm, we find λ on the order of 5 Å in good agreement with experimental observations on other samples.[41] Such a small value makes the classical approach of the indirect exchange mechanism by free carriers questionable, and indeed this is a subject of controversy.[42] In any case, it means that the range of magnetic interaction is shorter in heavily doped samples because of the resonant scattering of the holes on Mn that reduces the mean-free path with the consequence that T_C is lower than expected. The opposing effects of strong interaction and strong scattering may be at the origin of the difficulty to raise the Curie temperature up to room temperature in a diluted ferromagnetic semiconductor such as GaMnAs. The limitation of T_C by the reduction in the range of magnetic interactions is consistent with the exponent β that we have found. It seems thus doubtful that T_C might be increased up to room temperature in highly doped $Ga_{1-x}Mn_xAs$.

ACKNOWLEDGMENT

We thank Ludovic Largeau of the Laboratoire de Photonique et de Nanostructures (CNRS/LPN) for the x-ray measurements.

[1] T. Dietl, H. Ohno, F. Matsukura, J. Cibert, and D. Ferrand, Science **287**, 1019 (2000).
[2] J. Schliemann, J. König, and A. H. MacDonald, Phys. Rev. B **64**, 165201 (2001).
[3] J. L. Xu, M. van Schilfgaarde, and G. D. Samolyuk, Phys. Rev. Lett. **94**, 097201 (2005).
[4] R. Bouzerar, G. Bouzerar, and T. Ziman, Phys. Rev. B **73**, 024411 (2006).
[5] F. Tuomisto, K. Pennanen, K. Saarinen, and J. Sadowski, Phys. Rev. Lett. **93**, 055505 (2004).
[6] S. Das Sarma, E. H. Hwang, and D. J. Priour, Jr., Phys. Rev. B **70**, 161203(R) (2004).
[7] V. Novak, K. Olejnik, J. Wunderlich, M. Cukr, K. Vyborny, A. W. Rushforth, K. W. Edmonds, R. P. Campion, B. L. Gallagher, J. Sinova, and T. Jungwirth, Phys. Rev. Lett. **101**, 077201 (2008); L. Chen, S. Yan, P. F. Xu, J. Lu, W. Z. Wang, J. J. Deng, X. Qian, Y. Ji, and J. H. Zhao, Appl. Phys. Lett. **95**, 182505 (2009).
[8] S. Ohya, K. Ohno, and M. Tanaka, Appl. Phys. Lett. **90**, 112503 (2007).
[9] K. Ohno, S. Ohya, and M. Tanaka, J. Supercond. Novel Magn. **20**, 417 (2007).
[10] D. Chiba, Y. Nishitani, F. Matsukura, and H. Ohno, Appl. Phys. Lett. **90**, 122503 (2007).
[11] S. Mack, R. C. Myers, J. T. Heron, A. C. Gossard, and D. D. Awschalom, Appl. Phys. Lett. **92**, 192502 (2008).
[12] D. Chiba, K. M. Yu, W. Walukiewicz, Y. Nishitani, F. Matsukura, and H. Ohno, J. Appl. Phys. **103**, 07D136 (2008).
[13] J. Schliemann, J. König, H.-H. Lin, and A. H. MacDonald, Appl. Phys. Lett. **78**, 1550 (2001).
[14] J. König, T. Jungwirth, and A. H. MacDonald, Phys. Rev. B **64**, 184423 (2001).
[15] T. Jungwirth, J. König, J. Sinova, J. Kucera, and A. H. MacDonald, Phys. Rev. B **66**, 012402 (2002).
[16] X. Liu, Y. Sasaki, and J. K. Furdyna, Phys. Rev. B **67**, 205204 (2003).
[17] Kh. Khazen, H. J. von Bardeleben, J. L. Cantin, L. Thevenard, L. Largeau, O. Mauguin, and A. Lemaitre, Phys. Rev. B **77**, 165204 (2008).
[18] J. Smit and H. G. Beljers, Philips Res. Rep. **10**, 113 (1955).
[19] K. Khazen, H. J. von Bardeleben, M. Cubukcu, J. L. Cantin, V. Novak, K. Olejnik, M. Cukr, L. Thevenard, and A. Lemaitre, Phys. Rev. B **78**, 195210 (2008).
[20] S. M. Bhagat, H. S. Chen, and K. V. Rao, Solid State Commun. **33**, 303 (1980).
[21] A. Arajs, B. L. Tehan, E. E. Anderson, and A. A. Stelmach, Phys. Status Solidi **41**, 639 (1970).
[22] J. S. Kouvel and D. S. Rodbell, Phys. Rev. Lett. **18**, 215 (1967).
[23] M. N. Deschizeaux and G. Develey, J. Phys. (Paris) **32**, 319 (1971).
[24] M. E. Fisher, Rev. Mod. Phys. **46**, 597 (1974).
[25] O. Beckman, K. Gramm, L. Lundgeren, K. V. Rao, and H. S. Chen, Solid State Commun. **39**, 777 (1981).
[26] Y. Yeshurun, M. B. Salamon, K. V. Rao, and H. S. Chen, Phys. Rev. B **24**, 1536 (1981).
[27] P. Gaunt, S. C. Ho, G. Williams, and R. W. Cochrane, Phys. Rev. B **23**, 251 (1981).
[28] S. N. Kaul and M. Rosenberg, Philos. Mag. B **44**, 357 (1981).
[29] A. Mauger and M. Escorne, Phys. Rev. B **35**, 1902 (1987).
[30] H. Müller-Krumbhaar, J. Phys. C **9**, 345 (1976).
[31] S. J. Poon and J. Durand, Phys. Rev. B **16**, 316 (1977).
[32] A. Berger, G. Campillo, P. Vivas, J. E. Pearson, S. D. Bader, E. Baca, and P. Prieto, J. Appl. Phys. **91**, 8393 (2002).
[33] A. B. Harris, T. C. Lubensky, and J.-H. Chen, Phys. Rev. Lett. **36**, 415 (1976).
[34] I. M. Jiang, S. T. Lin, and C. H. Lo, J. Magn. Magn. Mater. **87**, 345 (1990).
[35] T. Mizoguchi and K. Yamauchi, J. Phys. Colloq. **35**, C4-287 (1974).
[36] A. Aharony and M. E. Fisher, Phys. Rev. B **8**, 3323 (1973); A.

D. Bruce and A. Aharony, *ibid.* **10**, 2078 (1974).
[37] S. N. Kaul, Phys. Rev. B **24**, 6550 (1981).
[38] M. A. Continentino and N. Rivier, J. Phys. C **10**, 3613 (1977).
[39] K. Binder and H. Müller-Krumbhaar, Phys. Rev. B **7**, 3297 (1973).
[40] P. G. De Gennes, J. Phys. Radium (Paris) **23**, 630 (1962).
[41] B. S. Sørenson, P. E. Lindelof, J. Sadowski, R. Mathieu, and P. Svedlindh, Appl. Phys. Lett. **82**, 2287 (2003).
[42] T. Jungwirth, J. Sinova, A. H. MacDonald, B. L. Gallagher, V. Novak, K. W. Edmonds, A. W. Rushforth, R. P. Campion, C. T. Foxon, L. Eaves, E. Olejnik, J. Masek, S.-R. Eric Yang, J. Wunderlich, C. Gould, L. W. Molenkamp, T. Dietl, and H. Ohno, Phys. Rev. B **76**, 125206 (2007).